



Journal of Agrometeorology

(A publication of Association of Agrometeorologists)

ISSN : 0972-1665 (print), 2583-2980 (online)

Vol. No. 27 (3) : 355-359 (September - 2025)

<https://doi.org/10.54386/jam.v27i3.3003>

<https://journal.agrimetassociation.org/index.php/jam>



Research Paper

Trend analysis of air surface temperature using Mann-Kendall test and Sen's slope estimator in Tunisia

IBTIHAJ S. ABDULFATTAH¹, JASIM M. RAJAB², MABROUK CHAABANE³ and HWEE SAN LIM⁴

¹Division of Human Resources, Mustansiriyah University Presidency, Baghdad, Iraq

²Department of Atmospheric Sciences, College of Science, Mustansiriyah University, Baghdad, Iraq

³Laboratory of Environmental Science and Sustainable Development LASED - University of Sfax - Tunisia.

⁴School of Physics, Universiti Sains Malaysia, 11800 Penang, Malaysia

Corresponding author email: hslim@usm.my

ABSTRACT

This study examines long-term (2003–2021) air surface temperature (AST) trends on monthly, seasonal, and annual patterns based on Atmospheric Infrared Sounder (AIRS) data from seven Tunisian sites using the MAKESENS model. Monthly AST patterns reveal a single peak, with January showing the lowest (280.29° K) and July the highest temperatures (312.40° K). Over 19 years, central stations exhibited stronger warming trends than desert and coastal regions. Tozeur showed the highest annual warming trend at 0.070° K year⁻¹, while EL-Borma recorded a slight cooling trend of -0.009° K year⁻¹. The Mann-Kendall test on AST data reveals significant monthly, seasonal, and annual trends. Positive trends were observed in January, February, April, May, November, and December, with negative trends in March, August, and October. Seasonally, warming trends was significant in winter and spring, with cooling trends in summer and autumn. Annual trends were predominantly positive across most stations. Warming was slower in summer and autumn along the Mediterranean coast but accelerated in winter and spring, particularly in continental areas. Regions south of 34° N warmed faster than northern and eastern regions, reinforcing the Mediterranean coastline as a climate change hotspot.

Keywords: Air surface temperature, MAKESENS model, Trend analysis, Mann-Kendall test

Since the industrial revolution, human activities have significantly affected Earth's climate, altering the atmosphere, land, and oceans. Increased GHG emissions and land-use changes have raised global air surface temperature (AST) and caused shifts in rainfall and other meteorological parameters (IPCC, 2021). Regional responses to anthropogenic climate forcing are complex and vary due to geographic and climatic factors. Satellite remote sensing has been widely utilized to investigate atmospheric, climatic, and gas properties (Rajab *et al.*, 2013). In recent decades, North Africa, the Mediterranean, and the Middle East have experienced accelerated increases in mean and maximum temperatures, alongside important reductions in precipitation (Ntoumos *et al.*, 2020).

Analyzing long-term meteorological time-series trends is essential for climate change research. Statistical methods, both parametric and non-parametric, are widely used to detect significant trends or abrupt changes in data. Non-parametric methods, such

as Mann-Kendall and Sen's Slope Estimator, are widely utilized to identify trends in climatic data (Aucahuasi-Almidon *et al.*, 2024; Landage *et al.*, 2024; Mekonnen *et al.*, 2024). The non-parametric Mann-Kendall test detects trends, while Sen's method quantifies them. The Mann-Kendall approach employs Z-statistics and S-statistics to estimate and evaluate trends in climatic datasets (Mann, 1945; Kendall, 1975; Sen, 1968). These techniques are effective for analyzing both monotonic and non-monotonic trends in time-series data.

This study employs trend detection methods to analyze long-term mean air surface temperature (AST) data from 2003 to 2021 at seven stations in Tunisia. The goal is to improve our understanding of temperature variability and trends through spatiotemporal analysis of monthly, seasonal, and annual AST trends.

Article info - DOI: <https://doi.org/10.54386/jam.v27i3.3003>

Received: 14 April 2025; Accepted: 23 July 2025; Published online : 1 September 2025

"This work is licensed under Creative Common Attribution-Non Commercial-ShareAlike 4.0 International (CC BY-NC-SA 4.0) © Author (s)"

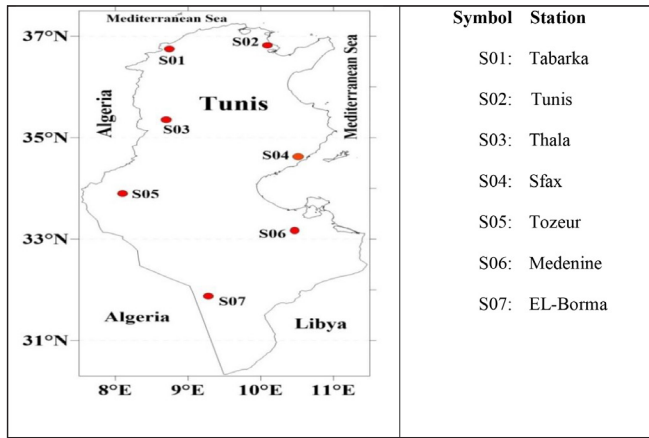


Fig. 1: Location map of study area

MATERIAL AND METHODS

Study area and data

Tunisia, located in North Africa between 7°–12°E and 32°–38°N, is bordered by Algeria, Libya, and the Mediterranean Sea (Fig. 1). Its topography includes a 1,298 km coastline, northern mountains, a central dry plain, and a semi-arid south transitioning to the Sahara. The South Mediterranean climate features cold, rainy winters and hot, dry summers. Coastal weather is heavily influenced by the Mediterranean, with rainy winters and warm, dry summers. Summer conditions are shaped by sea-land breezes, while westerly winds prevail in colder months.

This study analyzes the monthly (Daytime/Ascending) extended reconstructed AST dataset (Kelvin), version 7 over Tunisia from January 2003 to December 2023. The Level-3 dataset (AIRX3STM), with a spatial resolution of 1°x1° were sourced from NASA's website. The AIRS retrieval algorithm utilizes 103 channels for temperature, 25 for surface temperature, and 41 for water vapor, along with CO₂ absorption bands in the infrared spectrum, to estimate tropospheric temperature profiles over land with an accuracy of ±1 K at various atmospheric levels (Mohammed *et al.*, 2011; Jasim *et al.*, 2018).

Methodology

Trend detection in long-term monthly, seasonal, and annual AST series was conducted using the Mann-Kendall (Z) test and Sen's (Q) estimator across seven stations in Tunisia, utilizing AIRS Monthly AST data (AIRX3STM, 1°x1° resolution). MAKESENS 1.0, free software released by the Finnish Meteorological Institute in 2002, was used to determine and evaluate trends in AST time series. Specifically designed for analyzing trends in atmospheric chemical components, the software utilizes the nonparametric Mann-Kendall test to determine trend important and amplitude. The normal approximation test was applied by first calculating the variance of S using the following equation (Sen, 1968).

$$VAR = \frac{1}{18} \left[n(n-1)(2n+5) - \sum_{p=1}^q t_p(t_p-1)(2t_p+5) \right]$$

Where t_p is the total amount of data values in the p^{th} group

and q is the number of tied groups.

The test statistic Z_{mk} is calculated using the values of S and VAR (S) as follow

$$Z = \frac{S-1}{\sqrt{VAR(S)}} \text{ if } S > 0$$

$$Z = 0 \text{ if } S = 0$$

$$Z = \frac{S+1}{\sqrt{VAR(S)}} \text{ if } S < 0$$

The Z value is used to assess the strength and direction of a trend. A positive Z-score signifies an upward or increasing trend, whereas a negative Z-score indicates a downward or decreasing trend. For each station, monthly time-series (January 2002 to December 2021), were calculated the linear trends for each calendar month and averages of their seasonal and annual are by using the MAKESENS program and Sen's estimator. The Sen's test (Sen, 1968) is used to measure the magnitude of the linear trend slope in climatic time series. The slopes Q_i of all data set pairs are calculated as follows:

$$Q_i = \frac{(X_j - X_k)}{j - k} \quad \text{pour } i = 1 \dots N$$

where X_j and X_k are data values. The Q_i median is the Sen's slope, and calculated as below:

$$Q_{med} = Q_{((N+1)/2)} \quad \text{if } N \text{ is odd}$$

$$Q_{med} = [Q_{(N/2)} + Q_{(N+1)/2}] / 2 \quad \text{if } N \text{ is even}$$

A positive Q value implies an upward trend, whereas a negative value suggests a downward trend in the time series.

RESULTS AND DISCUSSION

Variation of monthly air surface temperature (AST)

Fig. 2 shows the monthly time series of variation of average AST values from 2003 to 2021 for seven provinces in Tunisia (Tunis, Sfax, Thala, Tabarka, Tozeur, Medenine, and El-Borma). The AST distribution for all stations exhibits a clear seasonal cycle, with temperatures peaking during the summer (June–August), due to intense solar radiation, and reaching their lowest values during the winter (December–February). Regional and station-specific variations in tendencies were documented. The average monthly standard deviation was $294.15^\circ \pm 14.02^\circ\text{K}$, with the northern region (above latitude 36°) showing the lowest variability, particularly near the coast. Seasonal AST variations are significantly shaped by weather and geographic factors.

All stations record peak AST in summer (July or August), generally exceeding 306 K (33°C), with Tozeur and El-Borma showing the highest values due to their arid and desert environments. Winter temperatures drop significantly in December and January, with Thala and Tozeur reaching the lowest values of around 284–288 K (11°C–15°C), reflecting their inland and arid conditions. Spring (March–May) and autumn (September–November) exhibit gradual warming and cooling, respectively, during seasonal transitions. Noticeable differences in AST between stations highlight regional climatic variations. Coastal stations (Tunis, Sfax, Tabarka) exhibit

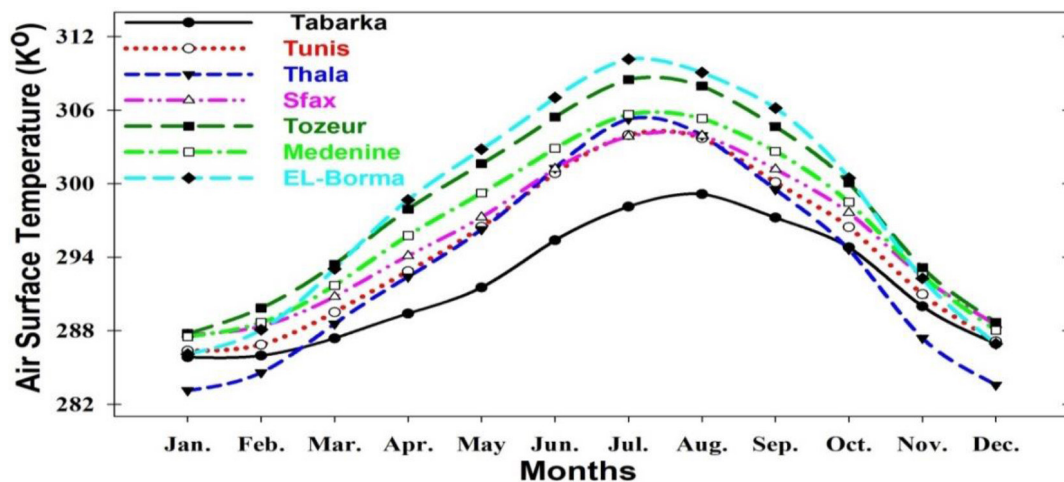


Fig. 2: Monthly variation of average AST for different stations of Tunisia

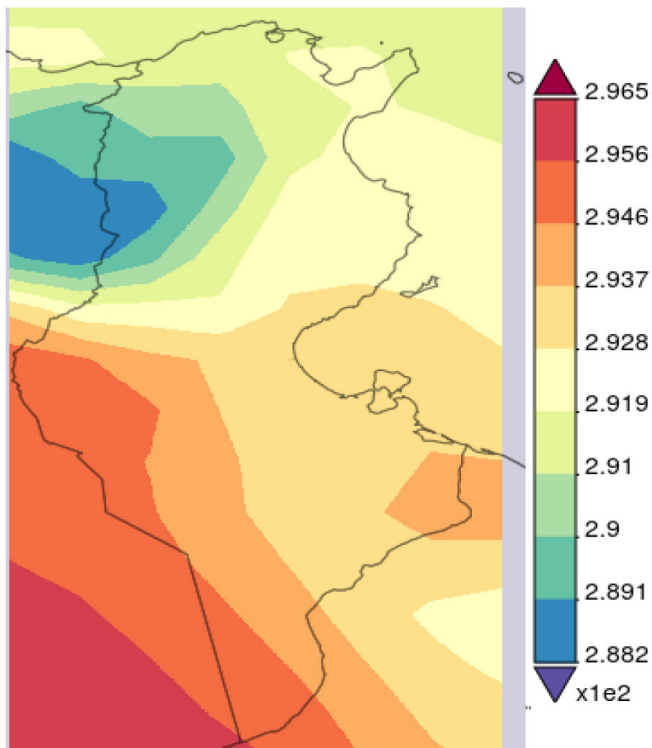


Fig. 3: Spatial distribution of average annual AST over Tunisia

milder temperature fluctuations, likely due to maritime influences that moderate extremes. In contrast, inland stations (Thala, Tozeur, Medenine, El-Borma) experience more pronounced seasonal variations, with higher summer peaks and lower winter lows. For instance, Tozeur and El-Borma record some of the highest summer temperatures, while Thala shows one of the most significant winter drops.

Throughout the year, AST values in Tunis and Sfax reflect a Mediterranean climate, with the lowest temperatures in the north (Tabarka, except October to March over Thala) and the highest in the south (El-Borma, except October to April over Tozeur). Global warming drives varying trends in absolute, mean, minimum, and maximum AST across different periods (IPCC, 2021). Analyzing

data from seven sites helps identify strategies to mitigate global warming's impacts across regions. Two sites exhibit a Mediterranean climate, while the others have diverse continental climates. The study aims to understand how rising AST trends affect ecosystems under global warming.

Spatiotemporal analysis of AST variability

Fig. 3 illustrates the annual spatial distribution of surface temperatures across Tunisia using a gradient color scheme, with cooler regions in blue and warmer areas in red/orange. The northern coastal areas near the Mediterranean Sea show the lowest temperatures, ranging from 303°K to 304°K, depicted in blue and light green. These cooler temperatures are likely due to the moderating influence of the Mediterranean Sea, which reduces heat compared to inland regions. The southern and central regions of Tunisia exhibit significantly higher temperatures, ranging from 310°K to 311°K, particularly in the arid desert areas of the southeast. These elevated temperatures reflect the Sahara Desert's harsh climate. In contrast, coastal areas experience milder temperatures due to the Mediterranean Sea's moderating effect, which acts as a heat sink to regulate temperatures. Inland areas, far from maritime influences, face much higher temperatures due to direct solar exposure and limited moisture to mitigate heating.

The topography elevation may influence cooler temperatures in northern Tunisia, potentially due to mountainous regions like the Atlas Mountains. However, proximity to the sea appears to be the dominant factor. Coastal areas, including a narrow band along the northern coastline, remain cooler due to sea breezes and the ocean's thermal inertia, which moderates temperatures. This cooling effect is particularly evident along the Mediterranean coastal plain. Moving inland from the coast, temperatures gradually rise due to the reduced influence of maritime air masses and the growing dominance of hotter, drier continental air.

The southern region, including the Sahara Desert, records the highest temperatures, attributed to sparse vegetation, low humidity, and minimal cloud cover, which maximize solar radiation absorption and limit evaporative cooling. The temperature gradient in Tunisia highlights a transition from a Mediterranean climate in

Table 1: Results of Mann-Kendall test for monthly, seasonal and annual AST trends in 2003–2021.

| Station | Tabarka | | Tunis | | Thala | | Sfax | | Tozeur | | Medenine | | EL-Borma | |
|-----------|--------------|---------------|--------------|---------------|--------------|---------------|--------------|---------------|-------------|--------------|--------------|---------------|--------------|---------------|
| Month | Z | Q | Z | Q | Z | Q | Z | Q | Z | Q | Z | Q | Z | Q |
| January | 1.05 | 0.080 | 1.12 | 0.101 | 0.39 | 0.029 | 1.12 | 0.121 | 2.45 | 0.241 | 1.40 | 0.130 | 1.61 | 0.154 |
| February | 1.40 | 0.161 | 1.33 | 0.107 | 1.33 | 0.155 | 0.88 | 0.066 | 1.47 | 0.125 | 0.63 | 0.064 | 1.05 | 0.067 |
| March | -1.26 | -0.044 | -1.05 | -0.049 | -1.51 | -0.065 | -0.98 | -0.050 | 0.21 | 0.014 | -0.84 | -0.037 | -1.54 | -0.099 |
| April | -0.21 | -0.009 | 0.11 | 0.010 | 0.04 | 0.003 | -1.44 | -0.069 | 1.23 | 0.041 | 0.77 | 0.025 | 0.46 | 0.023 |
| May | 0.28 | 0.018 | 0.91 | 0.055 | 0.35 | 0.060 | -0.04 | -0.003 | 1.61 | 0.120 | 1.82 | 0.114 | 1.26 | 0.102 |
| June | -0.63 | -0.028 | 0.21 | 0.011 | -0.77 | -0.061 | 0.25 | 0.013 | 0.95 | 0.061 | 1.12 | 0.064 | -0.67 | -0.023 |
| July | -0.35 | -0.007 | 0.42 | 0.025 | -1.12 | -0.051 | -2.14 | -0.078 | 0.77 | 0.068 | 0.00 | 0.006 | -1.51 | -0.133 |
| August | 0.00 | -0.001 | -1.86 | -0.077 | 0.21 | 0.023 | -2.14 | -0.080 | -0.21 | -0.009 | -0.53 | -0.041 | -1.40 | -0.106 |
| September | -0.07 | -0.008 | 0.11 | 0.005 | -0.98 | -0.074 | -0.11 | -0.003 | 2.80 | 0.120 | 1.79 | 0.078 | 0.00 | 0.001 |
| October | -2.24 | -0.155 | -2.38 | -0.154 | -2.17 | -0.193 | -2.31 | -0.141 | -1.54 | -0.099 | -2.45 | -0.156 | -2.42 | -0.277 |
| November | 0.70 | 0.046 | 0.42 | 0.018 | 0.11 | 0.005 | 0.18 | 0.002 | 2.03 | 0.070 | 0.00 | 0.000 | 0.00 | 0.017 |
| December | 2.07 | 0.094 | 1.75 | 0.072 | 2.14 | 0.117 | 1.40 | 0.043 | 1.61 | 0.085 | 1.12 | 0.048 | 1.05 | 0.062 |
| Winter | 2.38 | 0.119 | 2.03 | 0.095 | 1.61 | 0.102 | 1.96 | 0.097 | 3.08 | 0.177 | 2.17 | 0.094 | 2.10 | 0.097 |
| Spring | 0.42 | 0.014 | 0.35 | 0.008 | 0.00 | 0.002 | -1.40 | -0.027 | 1.40 | 0.038 | 0.70 | 0.029 | -0.07 | -0.003 |
| Summer | -0.32 | -0.024 | -0.63 | -0.021 | -0.84 | -0.045 | -1.47 | -0.036 | 0.98 | 0.068 | 0.21 | 0.007 | -1.68 | -0.071 |
| Autumn | -0.63 | -0.036 | -1.19 | -0.031 | -2.31 | -0.112 | -1.12 | -0.042 | 1.09 | 0.030 | -0.84 | -0.034 | -1.47 | -0.059 |
| Yearly | 0.63 | 0.011 | 0.49 | 0.007 | -1.12 | -0.023 | -0.63 | -0.013 | 3.36 | 0.070 | 1.12 | 0.025 | -0.42 | 0.009 |

the north to an arid desert climate in the south. High temperatures in the southern desert result from intense solar radiation, a dry atmosphere, and minimal cloud cover, exacerbating aridity, reducing agricultural productivity, and increasing water stress. In contrast, cooler coastal areas benefit from maritime air masses, supporting diverse ecosystems and human activities. While the north enjoys milder, humid conditions due to Mediterranean influences, the interior is dominated by hotter, drier continental air.

Monthly and seasonal trends of AST

Table 1 summarizes the monthly, seasonal and annual Mann-Kendall test results for AST data (2003–2021), revealing significant positive trends in November, December, January, and February, with Tozeur showing the highest Zmk value (2.45) in January. Positive trends were observed in April and May for most stations, except Tabarka and Sfax, this showed negative trends. Mixed trends were noted in other months: March had a positive trend only in Tabarka, while June saw negative trends in Tabarka, Thala, and El-Borma. Negative trends dominated July, September, and October (except Tunis, Tozeur, and Medenine) and August (except Thala). Tozeur, Tunis, and Medenine consistently showed strong positive trends, whereas Sfax, Tabarka, and El-Borma exhibited predominantly negative trends.

For seasonal analyses, Tozeur exhibits a strong positive trend ($Z = 3.08$, $Q = 0.007$) in winter, reflecting a statistically significant rise in temperatures, while other stations show weak or insignificant trends. In spring, Tozeur demonstrates a moderate positive trend ($Z = 1.40$, $Q = 0.038$), with other stations again showing weak or no significant trends. During summer, Tozeur displays a moderate positive trend ($Z = 0.98$, $Q = 0.068$), whereas El-Borma shows a strong negative trend ($Z = -1.68$, $Q = 0.071$), indicating a statistically significant decline in summer temperatures. In autumn, Tozeur records a moderate positive trend ($Z = 1.09$, $Q = 0.030$), while other stations exhibit weak or no significant trends.

Annually, Tozeur exhibits a strong positive trend ($Z = 3.36$, $Q = 0.007$), reflecting a statistically significant increase in AST over the study period. Medenine displays a moderate positive trend ($Z = 1.12$, $Q = 0.025$). In contrast, the other stations—Tabarka, Tunis, Thala, Sfax, and El-Borma—show weak or no significant trends, with El-Borma even demonstrating a weak negative trend ($Z = -0.42$, $Q = 0.009$).

CONCLUSIONS

The analysis revealed that coastal stations experience milder temperature fluctuations due to maritime influences, whereas inland stations demonstrate more extreme seasonal variations, shaped by their arid and mountainous landscapes. The monthly Mann-Kendall test revealed significant spatial variability in AST trends across Tunisia. While Tozeur consistently exhibits strong warming trends, other stations display weaker or even negative trends, underscoring regional disparities in climate dynamics. Tozeur emerges as the station with the most pronounced warming, both seasonally and annually, likely due to its location in southern Tunisia near the Sahara Desert, where arid conditions intensify warming effects. El-Borma stands out with a significant negative trend during summer and a weak negative annual trend, potentially influenced by local factors such as increased cloud cover, changes in vegetation, or microclimatic conditions. Many stations exhibit weak trends with p-values exceeding 0.05, suggesting that their temperature patterns are more likely driven by short-term fluctuations rather than long-term trends.

ACKNOWLEDGMENT

The authors wish to express thankfully acknowledge to the National Aeronautics and Space Administration (NASA) Goddard Earth Sciences Data Information and Services Centre (DISC) for the access of the AIRS data used in this paper.

Funding: This research was supported by Fundamental Research

Grant Scheme (FRGS) grant. Authors acknowledge the Ministry of Higher Education (MOHE) for funding under the Fundamental Research Grant Scheme (FRGS) (Reference Code: FRGS/1/2021/STG08/USM/02/2).

Conflict of interest: The authors declare no conflict of interest.

Data availability: Data are available on the giovanni website: <https://giovanni.gsfc.nasa.gov/giovanni/>

Authors contribution: **I. S. Abdulfattah:** Conceptualization, methodology, validation, formal analysis, original draft preparation, writing—review and editing the paper. **J. M. Rajab & M. Chaabane:** Conceptualization, methodology, validation, formal analysis, original draft preparation, writing—review, editing supervision. **H. S. Lim:** Conceptualization, methodology, validation, formal analysis, original draft preparation, writing—review, editing supervision.

Disclaimer: The contents, opinions and views expressed in the research article published in the Journal of Agrometeorology are the views of the authors and do not necessarily reflect the views of the organizations they belong to.

Publisher's Note: The periodical remains neutral with regard to jurisdictional claims in published maps and institutional affiliations.

REFERENCES

- Aucahuasi-Almidon, A., Cabrera-Carranza, C. and Garate-Quispe, J. (2024). Trend analysis and change-point detection of temperature and rainfall in southern Peruvian Amazon and its relation to deforestation. *J. Agrometeorol.*, 26(4): 425-430. <https://doi.org/10.54386/jam.v26i4.2687>
- IPCC. (2021). Summary for policymakers. Climate change 2021: The physical science basis. Contribution of working group I to the sixth assessment report of the intergovernmental panel on climate change. *Cambridge University Press*.
- Jasim Rajab, I. Abdulfattah, H. Mossa, and S. Sleeman, (2018). Spatial and temporal distributions of outgoing longwave radiation over Iraq: 2007-2016. *IOP Conference Series: Materials Science and Engineering*, vol. 454, no. 1: IOP Publishing, p. 012030.
- Kendall, M.G. (1975). Rank Correlation Methods. (4th ed.). Griffin, pp. 160
- Landage, R. S., Jadhav, V. T. and Patil, P. (2024). Trends of temperature and precipitation extreme indices in north Maharashtra. *J. Agrometeorol.*, 26(4): 442-446. <https://doi.org/10.54386/jam.v26i4.2735>
- Mann, H.B. (1945). Nonparametric tests against trend. *Econometrica*, 13:245-259.
- Mekonnen, E. F., Assefa, M. A. and Ayele, A. G. (2024). Trends in rainfall and temperature extremes during 1954-2019 in Addis Ababa, Ethiopia. *J. Agrometeorol.*, 26(4): 516-518. <https://doi.org/10.54386/jam.v26i4.2700>
- Mohammed Rajab, J., Matjafri, M.Z., Tan, F., Lim, H.S. and Abdullah, K. (2011). Analysis of Ozone column burden in Peninsular Malaysia retrieved from Atmosphere Infrared Sounder (AIRS) data: 2003-2009, IEEE International Conference on Imaging Systems and Techniques, 978-1-61284-896-9/11 IEEE, <https://doi.org/10.1109/IST.2011.29-33>, 5962213.
- Ntoumos, A., Hadjinicolaou, P., Zittis, G. and Lelieveld, J. (2020). Updated Assessment of temperature extremes over the Middle East-North Africa (MENA) Region from observational and CMIP5 data. *Atmos.*, 11(8):813.
- Rajab JM, Lim HS, and MatJafri MZ (2013). Monthly distribution of diurnal total column ozone based on the 2011 satellite data in Peninsular Malaysia, *The Egyptian J. Remote Sens. Space Sci.*, 16: 103-109. <https://doi.org/10.1016/j.ejrs.2013.04.003>
- Sen, P.K. (1968) Estimates of the regression coefficient based on Kendall's tau. *J. Amer. Stat. Assoc.*, 63(324):1379-1389.